Characterization of Defects in Fiber Composites Using Terahertz Imaging

A Thesis
Presented to
The Academic Faculty

By
Arungalai Anbarasu

In Partial Fulfillment
of the Requirements for the Degree
Master of Science in Electrical and Computer Engineering
The School of Georgia Institute of Technology

Georgia Institute of Technology
August 2008

Characterization of Defects in Fiber Composites Using Terahertz Imaging

Approved by:
Dr. **David S. Citrin**, Advisor
School of **Electrical and Computer Engineering**
Georgia Institute of Technology
Dr. **Stephen Ralph**
School of **Electrical and Computer Engineering**
Georgia Institute of Technology

Dr. **Douglas Denison**
School of **GeogiaTech Research Institute**
Georgia Institute of Technology

Date Approved: 05-Jun-2008

This dissertation is dedicated to my Family, Friends, Colleagues and Advisor for everything.

ACKNOWLEDGEMENTS

After all these years, I've got quite a list of people who contributed in some way to this thesis, for which I would like to express thanks.

This thesis would not have been possible without the kind support, the trenchant critiques, the encouragement, and the remarkable patience of my thesis advisor - Dr. David Citrin. I cannot thank him enough.

This work would not have been possible without the support and encouragement of my colleagues and friends - Dr. Prabha Chatterji, Dr. Abhinanda Sarkar, Dr. Sudeshna Adak, Dr. Vinay Jammu and Mr. Suchetana Shetty,

I would like to thank Dr. Michael Breit – GE Global Research, Munich for the use of his Terahertz CW system. I gratefully acknowledge the contribution of Thorbjeon Buck - GE Global Research, Munich who has provided precious information on the THz technology.

I remain indebted to my parents and little brother Aravazhi Anbarasu, mentors and professors. Their unflinching courage and conviction will always inspire me, and I hope to continue, in my own small way, the noble mission to which they gave their lives. It is to them that I dedicate this work for providing me the means to learn and understand.

TABLE OF CONTENTS

LIST OF TABLES

LIST OF FIGURES

LIST OF SYMBOLS AND ABBREVIATIONS

THz	Terahertz

SUMMARY

Terahertz radiation or T-rays or THz radiation refers to the region of the electromagnetic spectrum between approximately 100 GHz and 30 THz. This spectral region is often referred to as the “THz gap” as these frequencies fall between electronic (measurement of field with antennas) and optical (measurement of power with optical detectors) means of generation. THz measurements may yield useful information about the structural and chemical nature of the material inspected. Examples include detection of voids in materials and protein binding in biomolecules. This report provides an overview of THz measurements of defects in fiber composites. We find that it efficiently detects defects such as voids and delamination in glass fiber composites better than ultrasound, which was widely used for defect characterization in glass fiber earlier. Comparison of the existing methods with THz is presented in the report for characterization of defects.

CHAPTER 1

INTRODUCTION

Terahertz (THz) radiation or T-rays lies in the region of the electromagnetic spectrum between 100 GHz and 30 THz. This is the section overlapping the upper frequency range of the microwaves through the far infrared as shown in Fig. 1[8]. THz photons are emitted when a molecule changes its thermal, rotational or bending state. Energies involved in THz are much smaller. THz spectroscopy gives information regarding the molecular concentration as well as its physical condition (heat, pressure, speed etc.) THz waves have generated great interest in recent years because they interact with molecular rotations and with vibrations in condensed matter. Virtually every large molecule has a unique THz signature. Thus in principle, reflected or transmitted THz waves can be used not only to image an object but also to determine its chemical makeup. THz frequencies pass easily through many common clothing and nonmetallic packaging materials. The potential of these kinds of applications is driving intense research efforts to overcome the many hurdles that prevent the widespread use of THz waves. While other portions of the spectrum are already well established in material inspection applications, the properties of the THz band allow it to occupy a fairly new niche. Relatively, little study of the interactions between these wavelengths and matter has been undertaken. The reason for this was the difficulty in generating and detecting THz radiation. Recent advances in combining optical and electronic methods have allowed for the generation and detection of very high signal-to-noise ratio and high data acquisition rates of frequencies in the 0.1 – 3 THz range.[8]

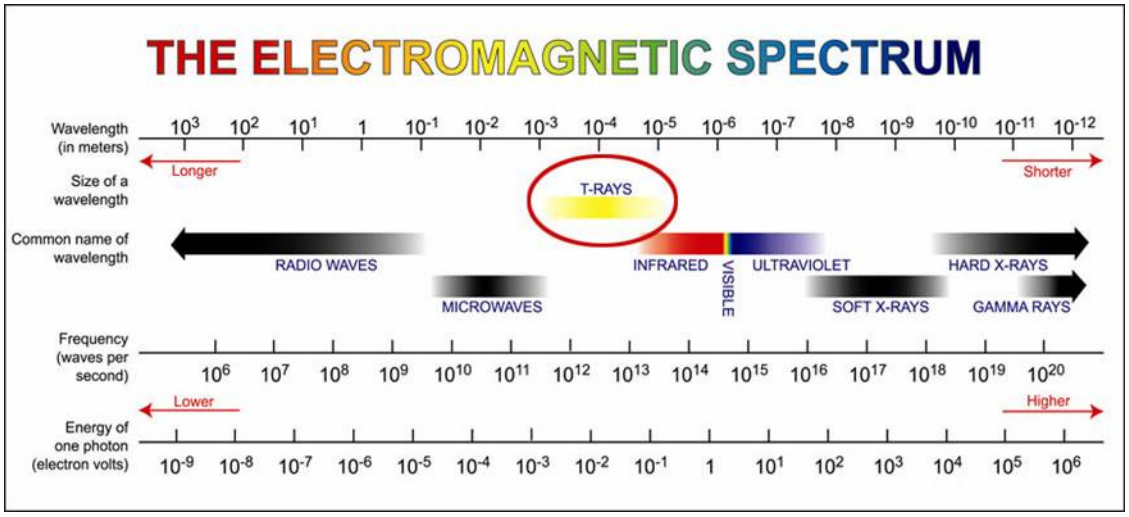

Figure 1: Electromagnetic spectrum illustrating the location of the THz band.

In this chapter, key issues impacting the use of THz radiation for imaging defects in fiber composites, current non-destructive evaluation techniques and the features of THz radiation are all reviewed, in order to provide a context for the current research objectives.

The thesis structure is outlined in the last part of this chapter.

1.1 Key Issue

This thesis focuses on the use of THz radiation to characterize fiber composites. The woven and continuous fiber is pre-impregnated with the given matrix (resin/ polymer) to form a fiber composite. Fiber composites typically consist of glass/carbon fibers in polymeric matrix. These composite materials provide higher strength to the structure that they are used in than the pure material form, for example in airplane wings, turbine blades etc.

The key issues impacting the structural integrity in fiber composite structures are buried voids and delamination. Voids are air or gas that has been trapped within the material. Voids are essentially incapable of transmitting structural stresses or non-radiative energy fields. It is important to know the existence of hidden voids in structures to avoid fatigue and other propagation-related application issues. Regardless of the resin, fiber type or fiber surface treatment, the interlaminar shear strength of composite decreases by about 7% for each 1% of voids up to a total void content of about 4%.

The condition of the separation of composite layers from each other is called delamination. Delamination leads to poor structural integrity and when undetected reduces the life of the composites.

The use of THz techniques is the basis of a class of potentially useful Nondestructive evaluation (NDE) techniques, as the defects of interest are frequently of the size scale of several THz wavelengths. Moreover, many of the materials to which these techniques are to be applied are opaque at near-infrared or optical wavelengths, but are transparent for THz fields. In addition, a number of widely deployed NDE techniques have low throughput or cannot be applied in situ; THz imaging may provide a set of methods to overcome these difficulties.

1.2 Current NDE Techniques

NDE is the use of noninvasive techniques to determine the integrity of a material, component, or structure to provide a quantitative measure of some characteristic of an object, i.e. inspect or measure without doing harm. In order to appraise the potential of THz radiation for NDE applications; it is in order to review its competition.

1.2.1 Ultrasound

Ultrasound is widely used in nondestructive testing to find flaws in materials. Frequencies of 2 to 10 MHz are common, but for special purposes other frequencies are used. Inspection may be manual or automated and is an essential part of numerous modern manufacturing processes. An example of an ultrasound tester is shown in Fig. 2. Most metals can be inspected as well as plastics and aerospace composites. Lower

frequency ultrasound (50 kHz to 500 kHz) can also be used to inspect less dense materials such as wood, concrete, and cement. The principle is that whenever there is a change in the acoustic impedance of the medium, the ultrasonic waves are reflected. Thus, from the intensity of the reflected echoes, the flaws are detected without destroying the material.

In ultrasonic testing, a transducer connected to a probe is passed over the object being tested. The transducer sends pulse waves into the surface of the object, returning an acoustic signal (echo) whenever an imperfection is encountered. The diagnostic machine may provide images of the acoustical properties of the object, and pulse readings, as well as the time it takes for the waves to return to the transducer, as shown in Fig. 2.

There are several commonly employed types of ultrasound scanning methods, as summarized in Table 1. A generic ultrasound setup is shown in Fig. 2.

Table 1: Ultrasound scanning methods.

A-SCAN	B-SCAN	T. M. SCAN
Amplitude Mode display	Brightness mode display	Time-motion mode display
1-D information	2-D information	Moving object information
Single fixed transducer	Single movable transducer	Single fixed transducer
Spike – Strength of echo	Brightness & size of dot – Intensity & strength of echo	X-axis – dots – position of defect depending on depth
Position – Penetration depth	Position – Penetration depth	Y – axis – movement of object
Detects position & size of flaws	Exact information of internal structure of flaw	

The advantages of NDE using ultrasound include sensitivity both to surface and to subsurface discontinuities, superior depth of penetration for flaw detection, high accuracy with respect to position, size, and shape of the defects, low hazard and very importantly, portable.

While ultrasound techniques are widely deployed for a variety of application, these techniques suffer from a number of limitations. They include the need of highly skilled and trained personnel. Moreover, irregular, rough, coarse grained or non homogenous parts, and linear defects oriented parallel to the beam cannot be clearly detected due some combination of to low transmission, small acoustical cross section for the given geometry, and high noise. Another important limitation is the coupling medium and reference standards requirements.

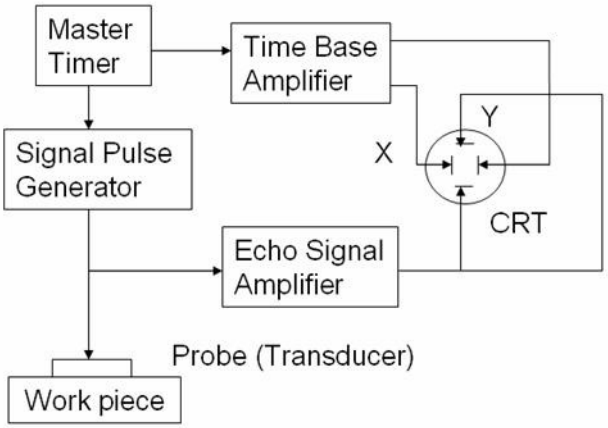

Figure 2: Schematic ultrasound setup.

The major limitation to conventional ultrasound is the necessity for the instrument and composite part to be interfaced with water. Laser ultrasonics, a no contact alternative, cannot supply an image of a part. It can only provide a vibration signature, which is then interpreted through rigorous mathematical techniques.[2]

1.2.2 Liquid penetrant inspection

Liquid penetrant inspection (LPI) is a widely applied and low-cost inspection method used to locate surface-breaking defects in many otherwise non-porous materials (metals, plastics, or ceramics). Penetrants may be applied to most non-ferrous materials, but for inspection of ferrous components, magnetic particle inspection is preferred for its subsurface detection capability. LPI is used to detect casting and forging defects, cracks, and leaks in new products, and fatigue cracks on in-service components. LPI is based upon capillary action, where a low surface tension fluid penetrates into clean and dry surface-breaking discontinuities.

The basic steps of liquid penetrant inspection are shown in Fig. 3. The surface to be inspected is cleaned thoroughly to remove all traces of dirt and grease. A brightly colored or fluorescent liquid is then applied liberally to the component surface and allowed to penetrate any surface-breaking cracks or cavities. The penetrant may be applied to the test component by dipping, spraying, or brushing. The time the liquid is allowed to soak into the material's surface is typically about 20 minutes, but may depend on the material studied and the penetrant employed. After soaking, the excess liquid penetrant is wiped from the surface and a developer applied. The developer is usually a dry white powder, which draws penetrant out of any cracks by reverse capillary action to produce indications on the surface. The developer helps to draw penetrant out of the flaw where a visible indication becomes visible to the inspector. Inspection is performed under ultraviolet or white light, depending upon the type of dye used – fluorescent or non-fluorescent (visible). These (colored) indications are broader than the actual flaw and are therefore more easily visible.[8]

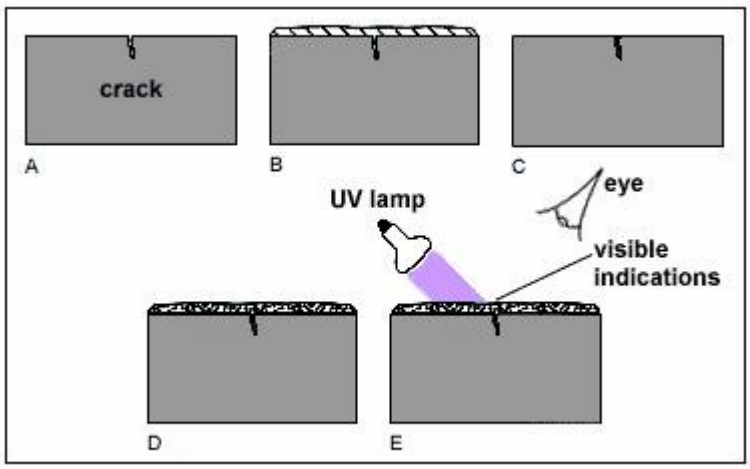

Penetrant testing:
A. Sample before testing;
B. Liquid penetrant applied;
C. Surplus wiped off leaving penetrant in crack;
D. Developer powder applied, dye soaks into powder;
E. View colored indications, or UV lamp shows up fluorescent indications.

Figure 3: Principle of liquid penetrant inspection.

This method is used only for surface defects and not buried defects. This is a major limitation of LPI.

1.2.3 Radiography

Radiographic testing (RT) or industrial radiography, is a NDE method of inspecting materials for hidden flaws by using the ability of short-wavelength electromagnetic radiation (high-energy photons) to penetrate various materials. Either an X-ray machine or a radioactive source (Ir-192, Co-60, or in rare cases Cs-137) can be used as a source of photons.The formation of an image of the test piece either on a photographic film or on a fluorescent screen due to X-rays or γ-rays passing through the test piece. The Lambert-Beere absorption law, which also applies to X-rays, is

$$I = I_o e^{-\mu x}$$

where I is output intensity, I_0 is input intensity, x is exposure and μ is a constant. Since the quantity of radiation transmitted through the material can be detected and measured, variations in the transmitted X-ray intensity are used to determine the thickness or composition of material. Fig. 4(a) illustrates an example of RT. The penetrating radiation is restricted to that part of the electromagnetic spectrum of wavelength less than about 10 nm.

X-rays are passed through the specimen under inspection. The spatial variations of the intensity absorbed by the specimen are recorded on photographic film, which is subsequently developed, thus providing spatial information on defect type and location.

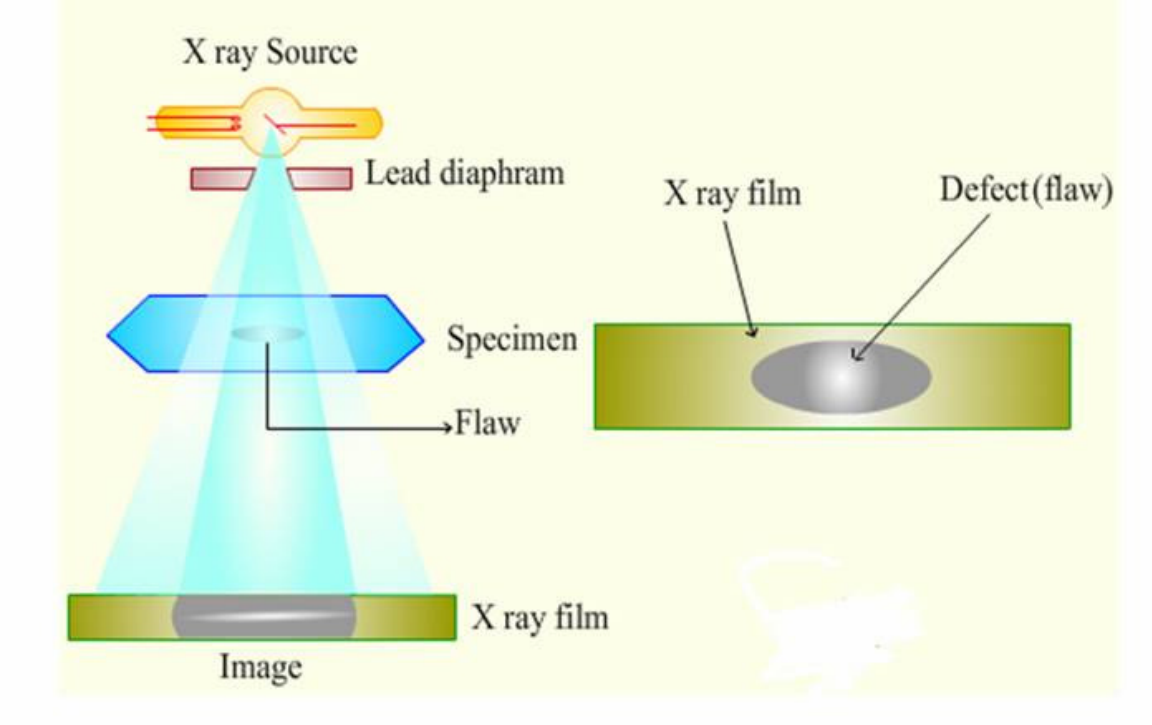

Figure 4(a): Schematic diagram of X-ray imaging system.

The use of x-rays is limited due to safety considerations related to the high-energy radiation, and the requirement to have access to both sides of a part. The scan size of the x-ray is also limiting, leading to an impractical scan time for inspection of a large aircraft part such as a rotor blade. X-ray equipment is a high cost item, with prices starting at approximately $250,000 per system.[2]

Fig. 4(b) shows impact delamination and crack damage of a composite using this technique. The great detail and accurate delineation of the damage extremities can be clearly seen. In conclusion it can be deduced that radiography is the best non-destructive testing technique for characterization of defects.[1]

Figure 4(b): A tetrabormoethane radiograph of impact damage of a woven glass fiber reinforced composite.

1.2.4 Comparisons of NDE methods for Fiber Composites

The foregoing discussion reviews a number of widely deployed NDE techniques. Table 2 summarizes these various techniques with regard to their application to fiber composites. [3]

Table 2: Comparison of techniques for fiber composites.

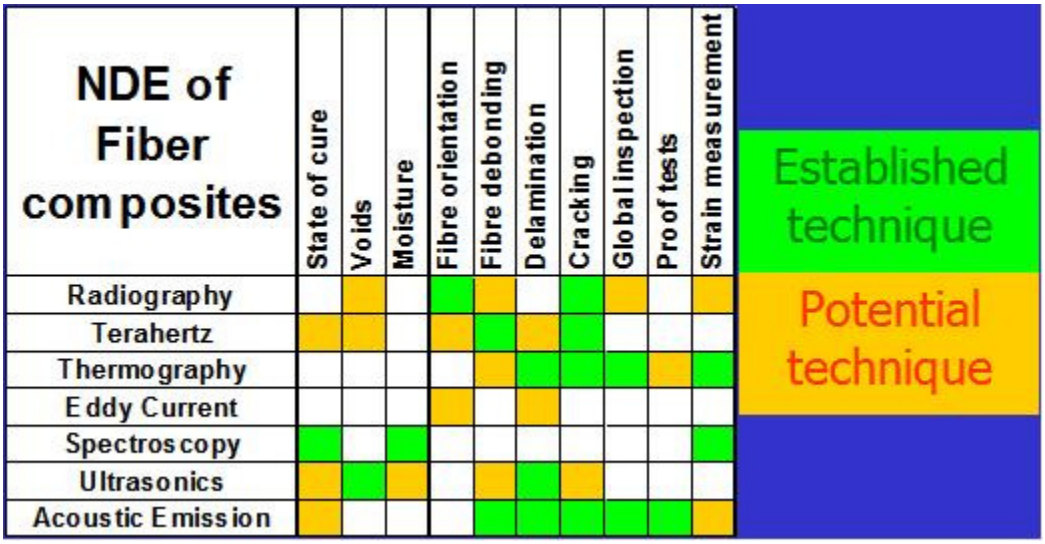

1.3 Pros and Cons of THz Imaging for NDE

THz radiations in some cases offer a great advantage over X-rays because they are in the far-infrared region, which is relatively low energy (on the order of one millionth that of X-ray photons). Thus, the photons are non-ionizing, making them safe biologically as well as non-damaging to materials at modest intensities.

Additionally, the THz region of the spectrum corresponds to a frequency in which many relevant molecular and lattice vibration and structural changes occur. THz allows the possibility of obtaining more than just positional or density information. Like positron emission tomography (PET), it can be used to assess the molecular activity in a medium as well as providing very high spatial resolution (300 μm). PET also involves tomography. One can imagine tomographic imaging modalities based on THz.). Instead of Compton scattering, pair production, and the photoelectric effects, THz radiation interacts with dielectric defects primarily by classical Mie scattering. This allows for a much simpler imaging setup without much scatter correction.

THz data may also be complementary to Raman spectroscopy. It also provides information on both high-frequency (just below IR) and low frequency vibrational modes; the latter are difficult to assess in Raman due to proximity to the visible excitation line. Moreover, THz techniques permit the direct observation of infrared-active modes, which in high-symmetry systems will not be visible in Raman spectroscopy. THz spectral

interpretation and instrumentation are in many cases similar to basic IR components and therefore may be relatively easy to understand.

As mentioned above, THz radiation is non-ionizing. This is a tremendous advantage when it comes to the safety of operators or for biomedical applications. It has transmission and reflection properties that are highly sensitive to the index of refraction $n(\omega)$ and absorption coefficient $\alpha(\omega)$ in the THz spectral range. THz radiation experiences far less Mie scattering (which scales as $\mu\lambda^{-4}$). THz radiation may be generated over a wide spectral bandwidth using ultra fast techniques. For example, high resolution and reproducible spectra of DNA macromolecules have been received in spectral range from 10 cm^{-1} to 500 cm^{-1}. THz techniques have been demonstrated with a high signal-to-noise ration (SNR) of 500-10,000: 1 for 1 second of acquisition time. THz radiation also provides a possibility of simultaneous acquisition of spectral, spatial, and temporal information with a time domain system.

THz radiation, however, undergoes strong attenuation in liquid water and atmospheric water vapor, although this could be an advantage in some cases, e.g. monitoring water-content in burns. The Fig 5 shows the atmospheric transmission The THz penetration length in non-conductive materials is ~ 2 mm. This implies that for most applications the sample must be very dry; otherwise, humidity becomes a highly detrimental factor (H_2O absorption at 1 THz is 235 cm^{-1}). It must also be noted that a lack of convenient and reliable solid-state sources such as LEDs, lasers, or electronic amplifiers has hindered THz development. Recently, however, a rich variety of THz sources and detectors are under development. We therefore expect the THz techniques will be much more widely deployed in the near future as various sources, detectors, and other devices are developed.[4]

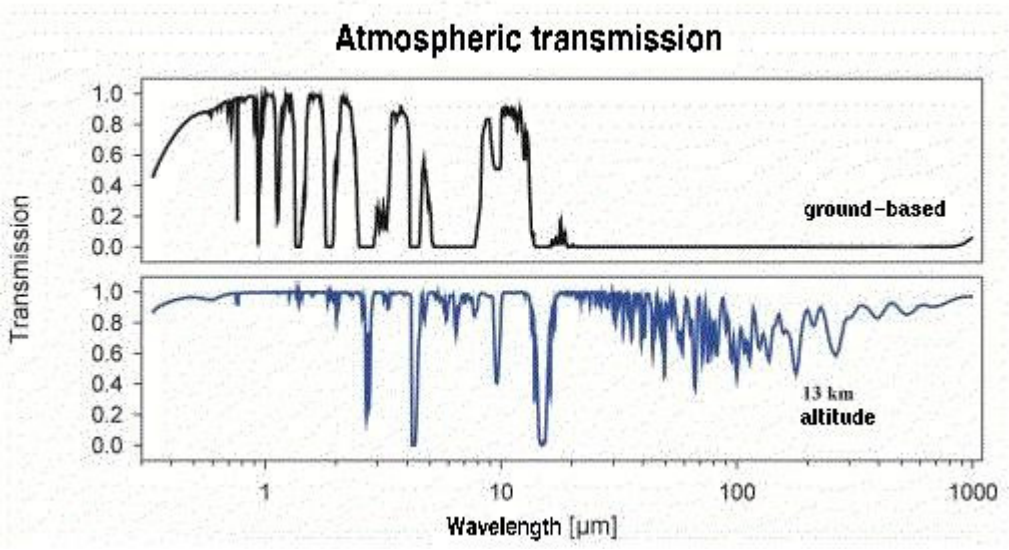

Figure 5: Atmospheric transmission in THz region.

1.3 Thesis Outline

We have thus reviewed various NDE techniques with an eye on their application to detecting buried defects in fiber composites. The rest of this thesis is organized as follows. Chapter 2 reviews the theoretical background to the use of THz techniques to image buried defects in fiber composites. The experimental approach to carrying out this imaging is discussed in Chap. 3. Results of our studies are presented in Chap. 4, followed by Chap. 5 that gives our conclusions.

CHAPTER 2

THEORETICAL BACKGROUND

2.1 Physics of THz measurements

Our work has focused on the use of a continuous wave (CW) THz system, and thus our discussion is confined to the spectral domain. The information/output signal in a cw system is stored in the form of intensity/contrast for the employed frequency. In general, there are three main physical effects to be taken into account in THz imaging, namely, absorption, reflection/transmission, and absorption.

One can assume in the systems of interest, that there are no further effects such as fluorescence, inelastic light scattering, etc.

We now discuss briefly the three main effects.

2.1.1 Absorption

Absorption is the energy transfer (coupling) from the THz wave to certain modes of the sample. For example, in small molecules, the modes, or energy states can be certain fundamental rotational modes. In polymers, these modes can be intramolecular vibrational modes, etc. In solids (crystals, ceramics), the states can be phonons or in presence of free charge carriers, energy transfer to the electronics system.

In general, as discussed for X-rays above, the intensity *I (x)* of a light beam propagating through a thickness of a material obeys the Beere-Lambert law,

$$I(x) \propto I_0 \exp(-\alpha.x)$$

where $I_0 = I(0)$ is the intensity of the beam prior to propagation through the thickness x of material and α is the absorption co-efficient. The Beere-Lambert law can be obtained by considering the optical intensity of a beam transferred to various modes of a material assuming that material is homogeneous and that the fractional energy transferred within a depth small *dx* of material is independent of the intensity of the beam. The energy transferred to the material shows up, via energy conservation, as energy lost from the beam leading to exponential attenuation. The absorption coefficient, moreover, may be highly sensitive to the frequency ν of the light beam, as density of modes in the material to which the light couples is likewise highly ν-dependent. In fact, this frequency dependence of α gives a means to characterize the chemical and physical properties of the medium.

Note that the Beere-Lambert law as stated above does not account for scattering of the beam by in homogeneities or for transmission and reflections of the beam at the surfaces of the medium.

2.1.2 Reflection/Transmission

Reflected waves are simply those waves that are not transmitted, but are reflected from the surface of the medium they encounter. When a wave approaches a reflecting surface, such as a mirror, the wave that strikes the surface is called the **incident** wave, and the one that bounces back is called the **reflected** wave .An imaginary line perpendicular to the point at which the incident wave strikes the reflecting surface is called the **normal**, or the perpendicular.

Given an incident beam, the fractional power T transmitted is related to the fractional power R reflected by the material

$$T = 1 - R$$

where, T is the transmission coefficient and R is the reflection coefficient. This feature can be used to measure sample thickness etc. Thus, the optical transmission sampled across an object can reveal optical paths containing less material than surrounding areas i.e., a void

2.1.3 Scattering

An electromagnetic wave incident on a random array of scattering particles loses energy through absorption and scattering by the particles, and is thus attenuated on propagation through the scattering region. Scattered radiation may be re-scattered repeatedly leading to complete diffusion. Scattering effects are particularly relevant in this spectral regime, where the wavelength, and the size and separation of scattering centers are often commensurable.

Pearce and Mittleman have determined that the statistics of a collection of scattering events provide a means to identify individual scattering events. However, when the same authors compared the mean free path for scattering through a dense collection of spheres with both exact (Mie) scattering and a quasi-crystalline approximation, typical differences of an order of magnitude are seen between experimental and theoretical values of the mean free path.

One additional optical effect is scattering. The phenomenon is well known from optics. There are several approximations/theories for the calculation of the angle distribution of the scattered radiation. In the limit $ka \ll 1$, the appropriate approximation is the so called Rayleigh-Scattering. In the limit $ka \ggg 1$, the appropriate approximation is the so called Mie-Scattering. [$k = 2\pi / r$; a is the radius of the scattering sphere]. Scattering produces signals in directions other than the incidence and reflection directions. [7]

2.2 Intensity/Contrast changes in THz imaging/Measurement due to the above effects

2.2.1 Transmission through sample without scatterer

The transmission through a sample without a scatterer is this expression, which neglects multiple reflections off. The exit and entrance faces of the sample can be modified to account for these effects.

$$I_a = I_o . T_a . T_2 . \exp(-\alpha . x)$$

where, T_a (T_2) is the front (back) interface transmission coefficient (given by the Fresnel formulae), I_0 is the incident intensity and I_a is the transmitted intensity. This equation neglects multiple reflections (Fabry - Perot effect), but can be modified to take this into account.

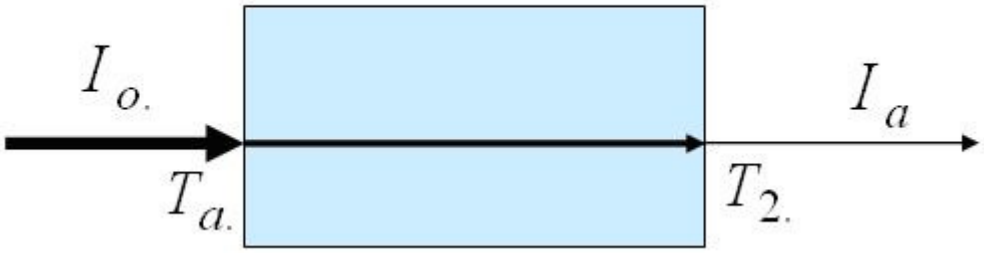

Figure 6: Absorption.

The changes in $T_a \,\&\, T_2$ due to carrier densities, changes in refractive index n and changes in α or x lead to changes in the intensity and thus for imaging, provide contrast.

2.2.2 Transmission through sample with large defect (compared to spot size)

The transmission through a sample with a large defect is this expression, which includes multiple reflections off. The exit and entrance faces of the sample cannot be modified to account for these effects.

$$I_z = I_o . T_{12} T_{21} T_{31} T_{13} \exp(-\alpha . x) \exp(-\beta . x)$$

where, $T_{12}, T_{21}, T_{31}, T_{13}$ are the various interface transmission coefficients defined in Fig. 7.

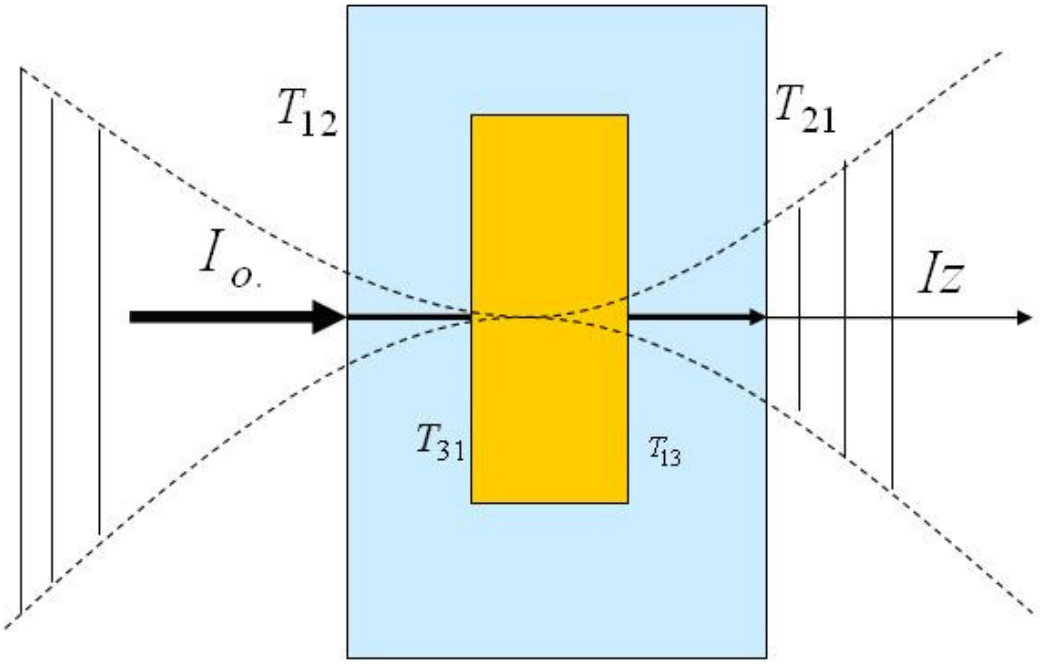

Figure 7: Scattering by large defect.

2.2.3 Transmission through sample with small defect

The transmission through a sample with a small defect, as shown in Fig. 8 is this expression, which includes multiple reflections off at the acceptance angles. That portion of optical intensity not scattered by the object is contained in the transmitted intensity I_s.

$$I_s = I_{o.} T_{12} T_{21} \int_{-\alpha_{accep\tan ce}}^{\alpha_{accep\tan ce}} \sigma_{scatter}(\alpha) d\alpha$$

where, $\sigma_{scatter}$ is the scattering cross section and $\pm \alpha_{accep\tan ce}$ are the acceptance angles.

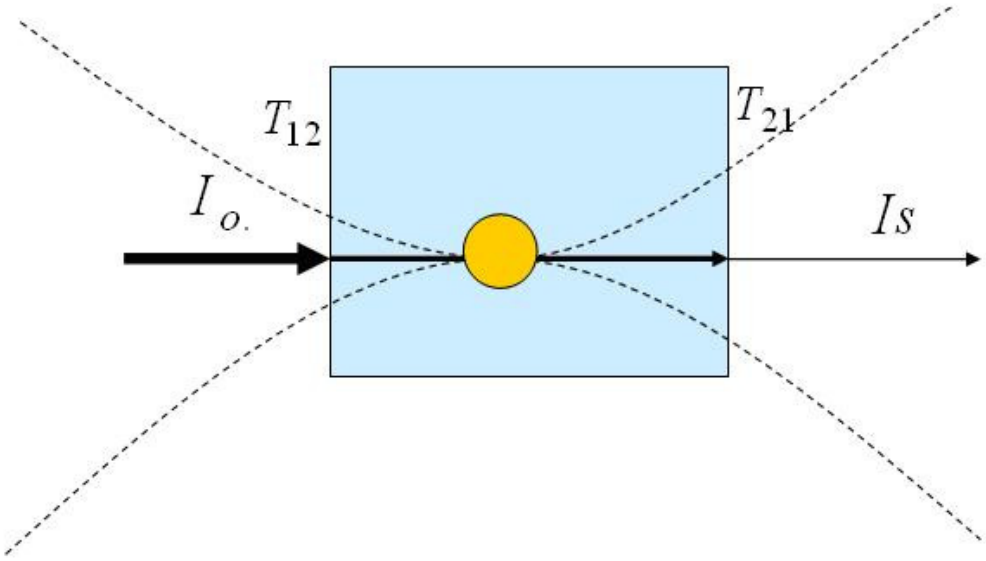

Figure 8: Scattering by small defect.

CHAPTER 3

TERAHERTZ EXPERIMENTAL SETUP

Broadly speaking, there are basically two types of THz radiation technologies: pulsed and continuous-wave (CW). A pulsed system is based on the use of electromagnetic pulses in picoseconds or sub-picoseconds duration. This pulse impinges on a sample and the transmitted or reflected waveform is coherently recorded in the time-domain. The frequency content can be retrieved by means of a Fourier transform. CW systems work at single frequencies or may be tunable and are faster and frequently more compact and simpler to operate. Several technologically deployed THz sources and detectors are summarized in Table 3. [5]

The THz sources and detectors available today are:

Table 3: THz Sources and Detectors.

Terahertz Sources:	*Terahertz Detectors:*
Thermal • Lamps/Black Bodies Electrical • Gunn Diodes/Mixers • *Backward Wave Oscillators* Optical / Laser Based • CO_2 Pumped Gas Laser • Optical Parametric Oscillator • Heterodyne C.W Photo-mixing • Terahertz Pulse Methods	Thermal • *Golay Cell* • Bolometer • Pyroelectric device Electrical • Photo-acoustic • Diode Optical / Laser Based • Terahertz Pulse Method

3.1 Components of the experimental THz CW system

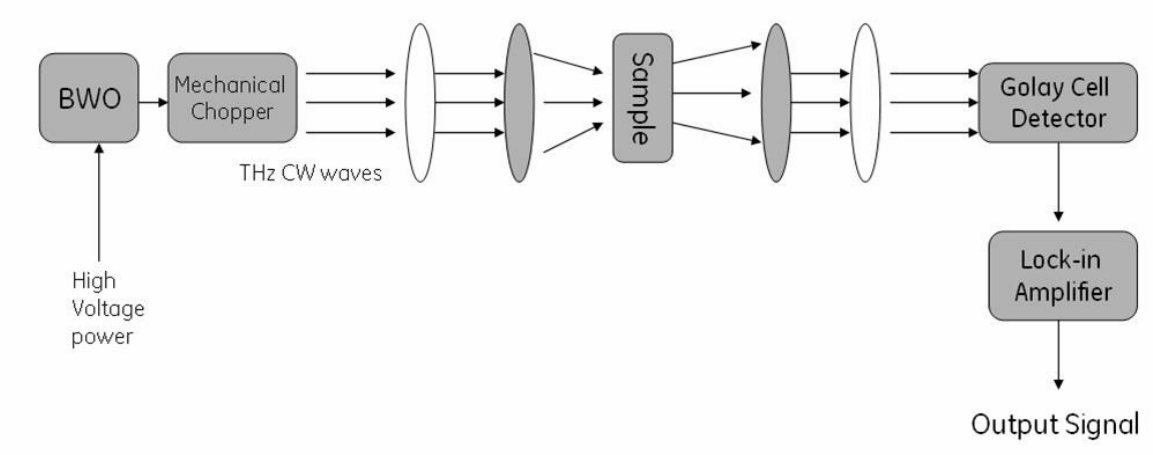

Figure 9(a): THz continuous-wave system.

As shown in Fig. 9(a), the CW system we employ uses a backward wave oscillator (BWO) as the source for the narrow-band THz radiation. A BWO, also called carcinotron or backward wave tube, is a device that is used to generate microwaves and THz radiation. It consists of a vacuum tube that provides 1 mW to 50 mW of power. Some types can produce frequencies in a range of 200 GHz to 1.4 THz. The BWO operates as follows. A heated cathode emits electrons that are focused by a strong magnetic field and drawn toward the anode through a comb like decelerating structure. As a result, an electromagnetic wave is produced that travels in the opposite direction (hence the name) and couples into a curved waveguide that takes it out into free space. The output frequency depends on the electron speed, which is determined by the voltage applied between the electrodes. Due to the high quality wavefront produced, BWO's find use as illuminators in THz imaging. A mechanical chopper is present after the BWO to modulate the THz energy at a low frequency. Convex lenses focus the beam and two geometries can be implemented: transmission and reflection. Common lens materials include Teflon and polyethylene. Teflon is an excellent material for these studies since its absorption coefficient is quite low at terahertz frequencies. Also, the refractive index of Teflon, η_{PTFE} = 1.35 - 1.38 nearly independent of frequency throughout the spectral range of the measurements. The refractive index of polyethylene, η_{HDPE} = 1.54. A Golay cell detector is used to detect the THz signal after interacting with the sample.

A **Golay Cell**, or **Golay Detector**, is a type of radiometer in which light is absorbed onto a plate in contact with a gas chamber, which heats the gas and causes it to expand against a diaphragm. A measurement of the diaphragm, typically with a strain gauge, determines the amount of radiation. Golay Cells are extremely efficient and were a standard method of detecting infrared radiation until the recent introduction of various solid state detectors. The **lock-in amplifier** then uses a very narrow band-pass filter (in the frequency domain representation) to select the signal modulated at the chop frequency.

Essentially the lock-in amplifier measures an AC voltage (or current) and gives an output in the form of a DC voltage proportional to the value of the AC signal being measured. It is called an "amplifier" because the DC level at the output is usually greater than the AC level at the input and is termed "lock-in" because it locks to and measures the particular frequency of interest ignoring all other signals at the input. The heart of the lock-in amplifier is a phase sensitive detector, sometimes known as the demodulator. It is this part of the instrument that demodulates the frequency of interest and it should be noted that its output is also a function of the relative phase angle between the input signal and the associated reference signal. It follows, therefore, that the lock-in amplifier can also be used to measure the relative phase relationship of two signals of the same frequency. The time constant of the lock-in amplifier was set to 10 ms for these measurements. Allowing a factor of 3 between the pixel time and the time constant, this means a scanning speed of 33 pixels/s. This is fed into the imaging system. The acquisition times for these samples vary from 5 - 10 minutes.

The specific THz CW system on which the data for this study was collected resides at GE Global Research, Munich, Germany and is shown in Fig. 9(b).

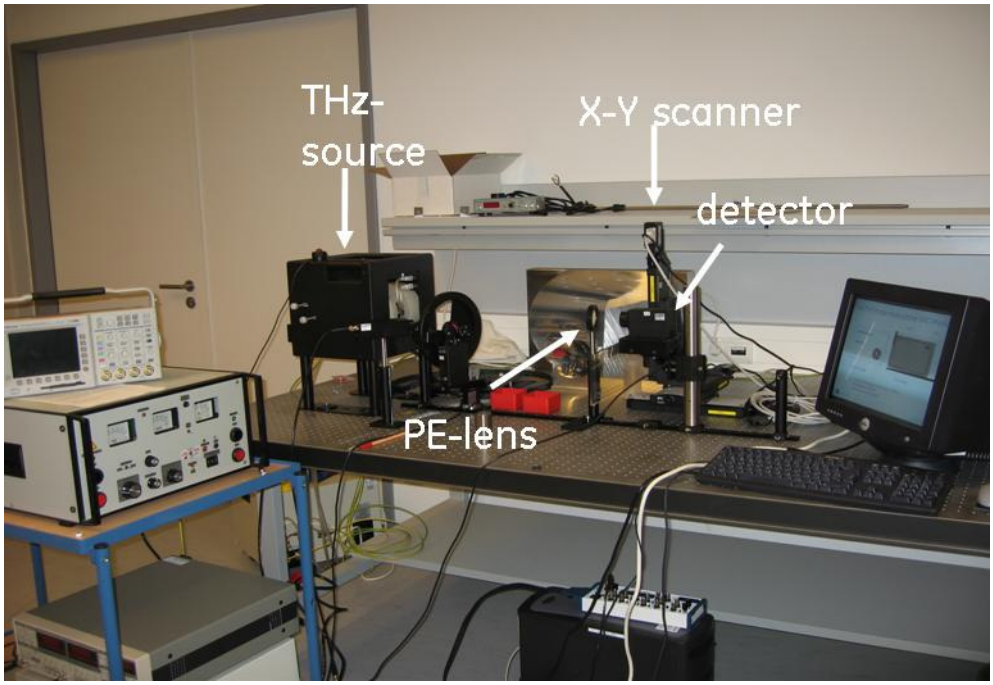

Figure 9(b): Photograph of the experimental setup.

3.2 Process

The THz transmission setup can in practice only be applied to samples that are relatively 15- 90 % transmissive in the THz region. Therefore, it is first necessary to find the transmission of the fiber composite samples in the THz frequencies.

3.3 Image Processing

In the CW system, shown in Fig. 9(a) the intensity data from the lock-in amplifier are simply stored in a matrix, which can be directly converted to a raster image. A raster scan is the pattern of image detection and reconstruction in computer, and is the pattern of image storage and transmission used in most computer image systems. In a raster scan, an image is cut up into successive pixels along scan lines. Each scan line can be transmitted as it is read from the detector. After each scan line, the position of the scan line is advanced, typically downward across the image in a process known as vertical scanning, and a next scan line is detected, transmitted, stored, retrieved, or displayed. This ordering of pixels by rows is known as raster order, or raster scan order. In the CW images, voids are identifiable as bright spots with dark borders, as a result of less material within the void that absorbs the radiation and reflection and interference at the edge, respectively. In our test samples, delaminations were formed by the presence of a thin piece of ceramic on the substrate in the place of the glue that would normally bind the two.

3.4 Sample Preparation

The design for the experimental samples was provided to the GE Plastics division at Bangalore who fabricated the samples for the experiments. A brief explanation how the sample was prepared is discussed in this sub section.

3.4.1 Molded sample with voids

Polymers can be converted to various shapes using various processing techniques. Most of the techniques involve heating the polymer to its softening point and then using the processing technique to obtain the desired shape. Polymers have different softening points based on its molecular structure. When the polymer is heated to the softening temperature the polymer chains gain mobility and cause the polymer to expand. When cooled the chain lose the mobility and the polymer shrinks back to its original state.

Injection molding of polymer involves heating the polymer and pressurizing the softened polymer into a mold. The polymer cools down in the mold to take the geometry of the mold. During the cooling stage, the outer layer in contact with the mold cools first and the cooling progresses to the center of the part. Due to the mode of cooling, the center section of the part stays warmer for a longer time. Also since the cooling involves volumetric shrinkage, voids are formed in the center of the part (along the thickness). To overcome the voids formation, excess polymer is held under pressure till the gate freezes, after which additional pressure or time does not help reduce the voids. The excess polymer held under pressure to over come the voids is called ‘cushion’.

The molding process parameters are designed to completely pack the part. When the process parameters are incorrect or when the process is unstable, various defects are observed and voids could be one type. Visual detection of voids is frequently difficult. Some of the techniques used to detect voids are, tapping, part weight, and X-rays.

For this study, the optimum molding conditions were first designed for the part. To reach the desired shot size, the shot size was by progressively increasing until the part was completely filled while keeping the pack and hold time and pressure at zero. Once the part was completely filled, the pack and hold time and pressure were increased until the part obtained have zero surface defects. Once the process is established, the shot size was reduced by 5% and reduces the hold time and pack time to zero. This gives parts that have sink marks and voids along the edges of the part.

3.4.2 Fabricating sandwich structure

Sandwich structures can be created in polymeric system by bonding substrates. The bonding of the substrates can be carried either by heating the bonding area or by the use of adhesive.

While bonding substrates with an adhesive or solvent, improper process controls could lead to voids at the interface. If the layers are transparent the voids could be visible. In case of opaque or non-transparent materials, the voids would remain unnoticed,

To analyze the defects at the interface two plaques of polycarbonate were molded of which one was transparent. In this study the molding process for the transparent and the nontransparent plaques was designed to obtain a completely packed, defect free part.

Holes of various diameters ranging from 0.5 mm – 3 mm were drilled in the nontransparent substrate. The holes were also drilled to various depths ranging from 1mm – 3mm. Also to simulate surface defects, areas of the plaque were scored. Also fine nicks were made on the surface to replicate small voids.

Di-chloro Methane (DCM) was then applied on the substrate of the nontransparent plaque which had the above-mentioned features. The transparent plaque was then laid and the two substrates were held under pressure for 1 hour. Since DCM softens Polycarbonate, the polymer chains at the interface of the two substrates diffuse and on the volatilization DCM the two plaques are bonded to each other.

The areas that have the induced imperfections will not be bonded and these areas represent the voids formed during solvent bonding of polymers.

The photographs of the samples are shown in Fig. 10.

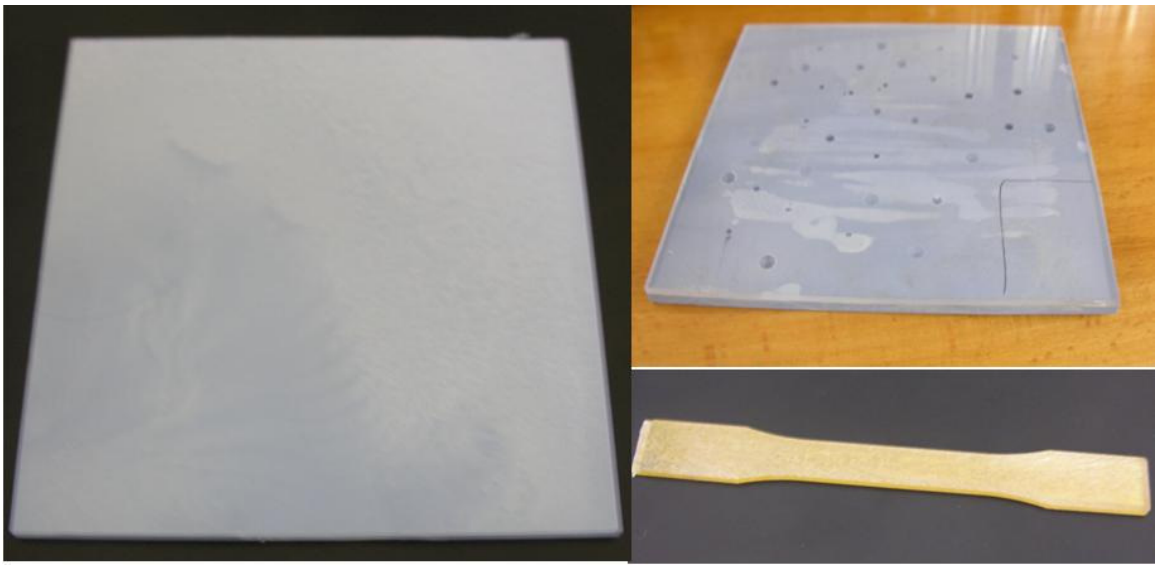

Figure 10: Photographs of fiber composites samples.

CHAPTER 4

RESULTS

4.1 Transmission Characteristics of the samples

The THz transmission of the fiber composite samples, the details of which are discussed below of different composition is shown in Fig 11.

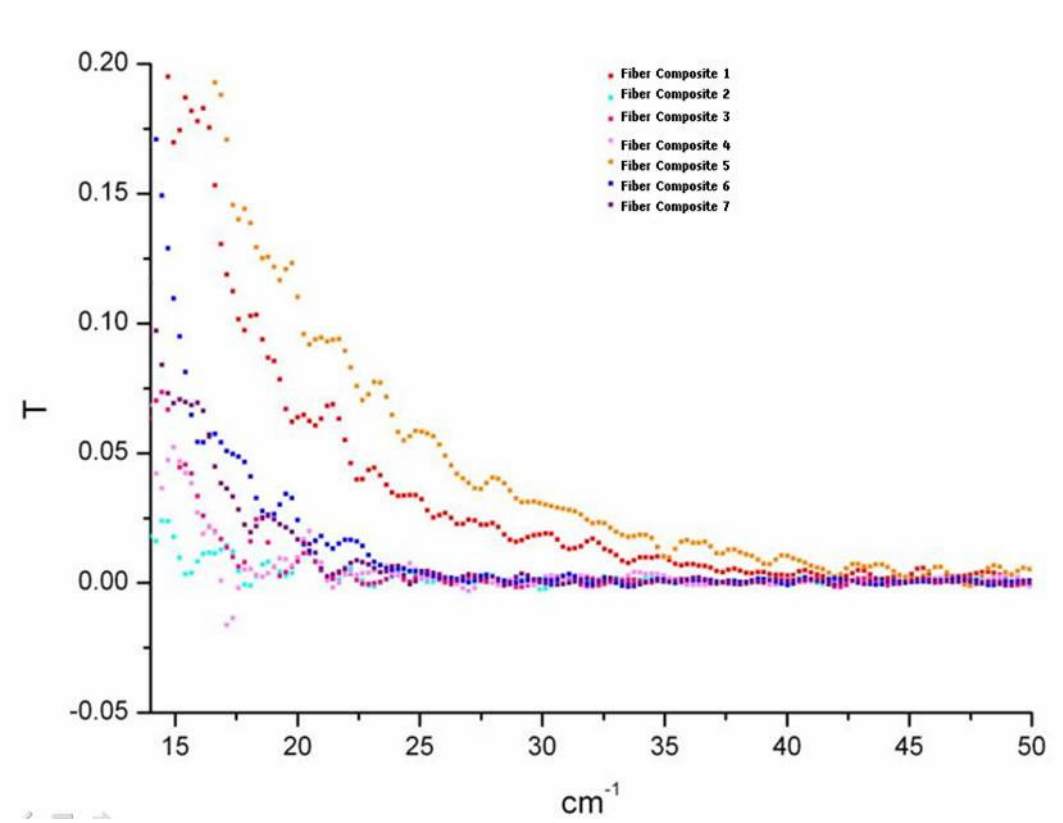

Figure 11: Transmission of various fiber composites samples.

Fiber Composite 1, 5, and 6 show 15 - 20% transmission at 15 cm^{-1} - 20 cm^{-1} wave number. These samples correspond to glass fiber composites. Fiber composite 2 shows only a 2.5 % transmission, which emphasizes on the fact that THz measurements cannot easily be applied to it. This composite is made of a conductive material (graphite).

The defects to be detected within a sample can be mainly divided in two types: voids and delaminations. Voids are basically air bubbles trapped inside the foam during the manufacturing process. A delamination is a detachment of two adjacent sprayed layers and is less common. Voids appear as dark shapes with light interiors, corresponding to the scattering and interference at the edge of the feature and enhanced transmission due to

the lack of material in the interior, while a delamination appears as a dark area corresponding also to scattering by the air layer.

4.2 Fiber composite 1

The *fiber composite 1* with dimensions 165mm x 20mm(neck=13mm) x 4mm had buried voids of around 100 microns. The sample is molded neat polycarbonate with (3%) glass fibers in random configuration. A resolution of 30 microns can be achieved.

The result from the THz transmission image is shown in Fig 12.

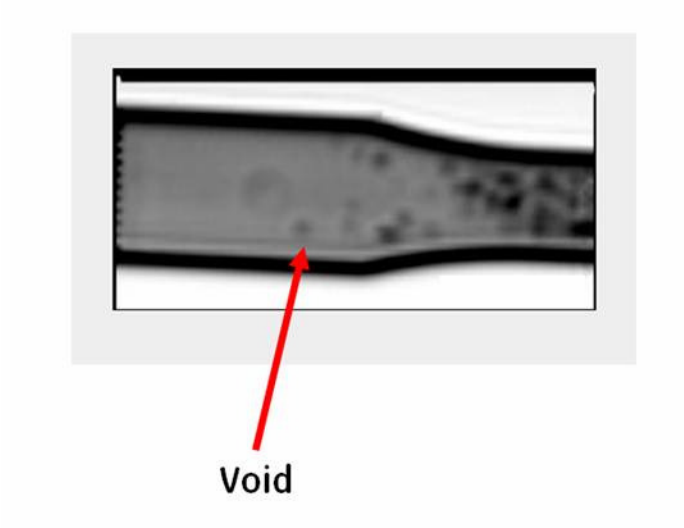

Figure 12: Fiber Composite 1 - Glass fiber composite (165mm x 20mm(neck=13mm) x 4mm) with buried voids.

The discrepancy between the THz image and the known defects could be due scaled up or scaled down images affects the visual interpretation of the defect's original sizes. Edges do not appear smeared or sometimes do not appear as edges at all. Due to the long coherence length of the emitted radiation, interference effects are likely to occur at the edges, between surfaces, etc. This could lead to poor interpretation of results. An example response of a theoretical diffraction by an abrupt edge is shown below in Fig. 13.

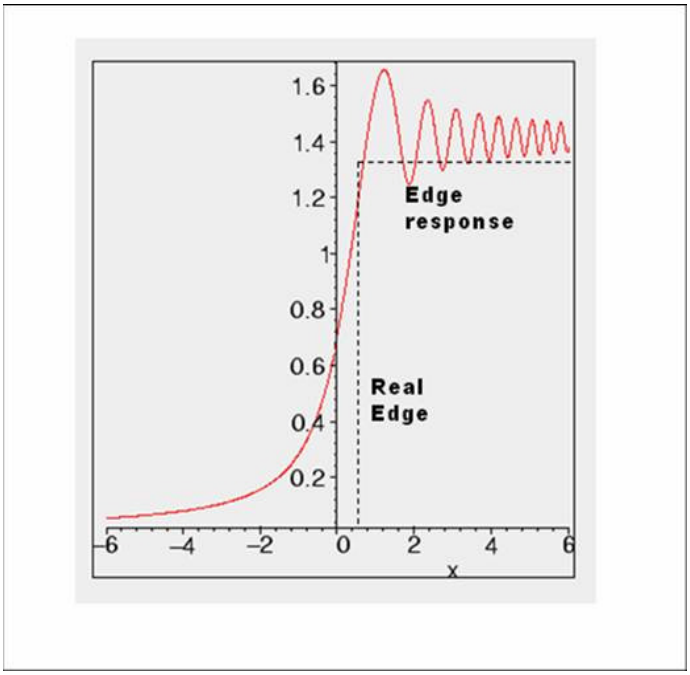

Fig. 13: Intensity of the edge response vs. real edge.

4.3 Fiber composite 5

The *fiber composite 5* with dimensions 150mm x 150mm x 5mm had buried voids of around 100 microns and less sized near the edges of the sample. These voids are placed at very small distances 5 microns between each void. The sample is a Polycarbonate + 20% glass fibers. The parts were molded with low packing pressure. The alignment of the glass fibers was along the length of the part (parallel to the two edges which are not cut). A resolution of 30 microns can be achieved.

The result from the THz transmission image is shown in Fig 14.

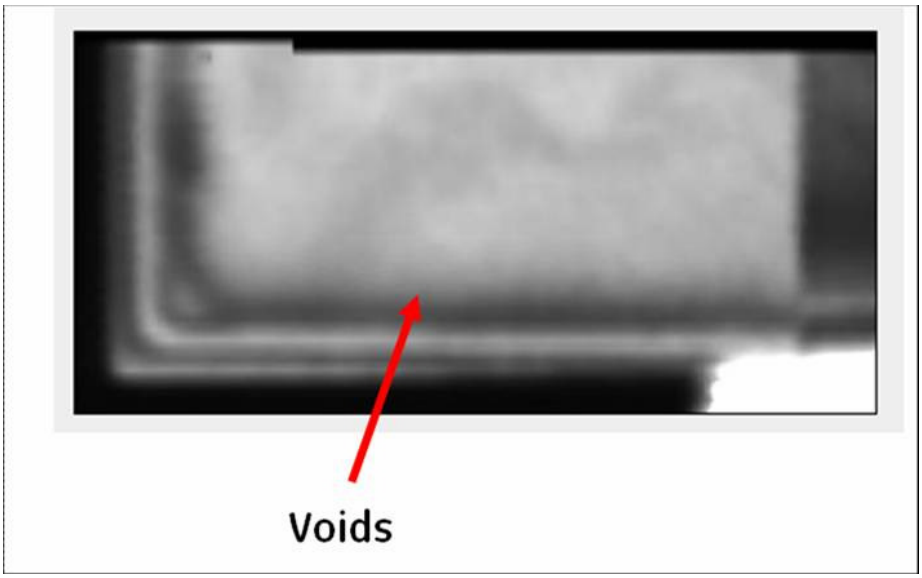

Figure 14: Fiber Composite 5 - Glass fiber composite (150mm x 150mm x 5mm) with buried voids in the edges.

The discrepancy between the THz image and the known defects could be due to the voids being placed very close, they become non-detectable. Thus the exact defect cannot be seen instead the whole area shows an intensity difference. This is due the Mie scattering of the THz signal due to the voids as shown in Fig 15.

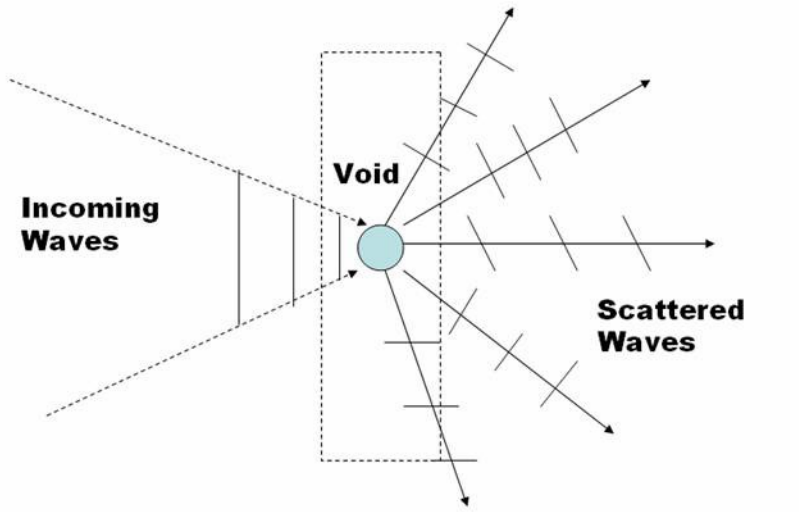

Figure 15: Mie scattering phenomenon.

4.4 Fiber composite 6

The *fiber composite 6* with dimensions 150mm x 150mm x 5mm (Layer 2= 3mm) had buried voids of 3 mm and lesser sized. This composite is also layered and has marked delamination between the layers. The sample is the Polycarbonate + 20% glass fibers.

The parts were molded with high packing pressure. The alignment of the glass fibers will be along the length of the part (parallel to the two edges which are not cut). A resolution of 30 microns can be achieved for voids and 10 microns for delamination.

The result from the THz transmission image is shown in Fig 16.

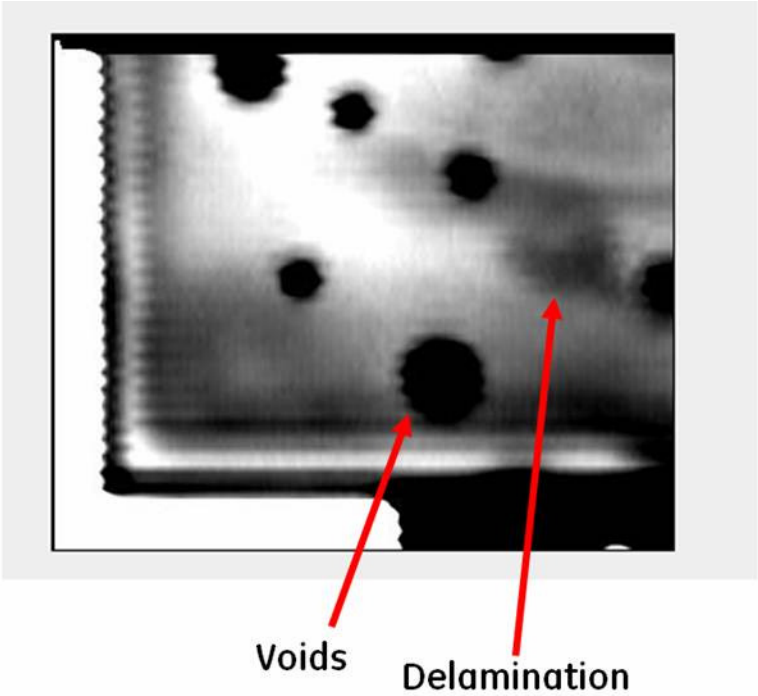

Figure 16: Fiber Composite 6 - Layered Glass Fiber composite (150mm x 150mm x 5mm (Layer 2= 3mm)).

The discrepancy between the THz image and the known defects could be since edges do not appear smeared or sometimes do not appear as edges at all. This is due to the coherence effect.

4.5 Fiber composites Imaged with THz and Ultrasound

The same samples underwent an imaging process through an ultrasound imaging system, which has the following details.

The ultrasound flat transducer was operated in the frequency of 10 MHz at a scanning resolution of 0.5 mm and scan dimension of 100 by 22 mm. For example, in the image in Fig. 17a and Fig. 17b there are 200 by 44 points.

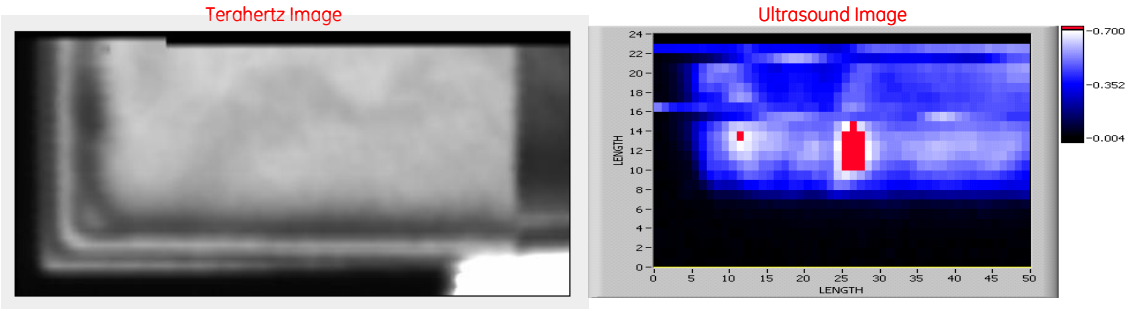

Figure 17a: Fiber composite 5 imaged in THz and ultrasound.

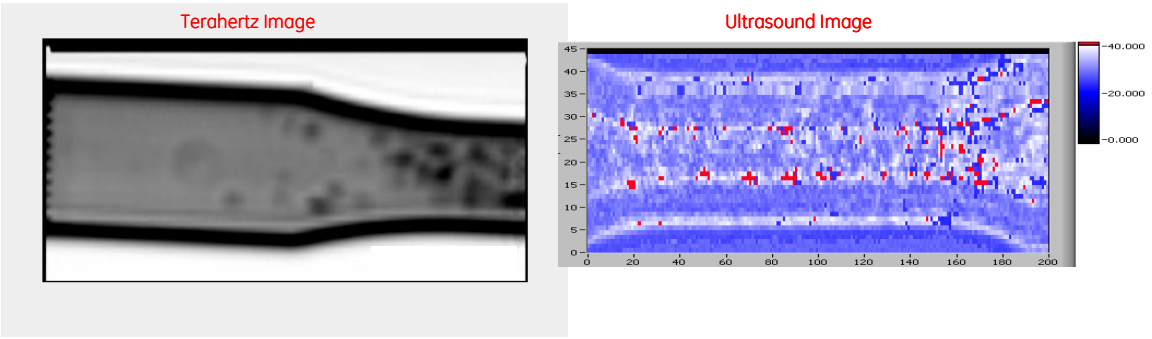

Figure 17b: Fiber composite 1 imaged in THz and ultrasound.

The example above clearly shows the resolution of imaging on THz is higher than that of the ultrasound in terms of clear void detection in the fiber composites.

CHAPTER 5

ANALYSIS OF RESULTS

5.1 Errors possible in the measurement

There are a number of possible sources of error. Lenses are aligned for each case at specific distances for good focus. Alignment is done by the experimentalist and to some extent depends on level of expertise. This induces a large amount of human error. Use of reflection optical elements instead of lenses, ensure correct focusing as well as easy and precise tracking with visible light. Likewise, the sample position must be well known.

5.1.1 Reflections

CW systems in normal reflection geometry show a common problem related to the generation of an interference pattern due to the interference between the incoming beam and reflected beams from the sample, lens and other surfaces. In order to reduce such effect, the system incorporates a compensating mirror with the intention to send part of radiation reflected from the beam splitter again to the detector in order to cancel the reflection coming from the lens, which is the main reflective surface besides the sample itself.

5.1.2 Etalon Effect

One of the problems that occur when one is imaging with such a highly coherent source is the presence of the etalon effect. Its origin is the back-and-forth propagation of the THz wave between two surfaces that come into the beam's path and form a resonance cavity. The effect manifests itself as bright and dark interference fringes that appear in the image. The reflecting surfaces can be the sample faces, the detector, or the source, such that they cannot be easily eliminated. One method for reducing the etalon effect is to reduce the reflection on the surfaces involved, for example, by tilting one of them, to direct the reflected waves out of the system for the detector. Tilting the sample leads to a result like the one shown in Fig.18 in which a cancer-tissue sample was scanned with and without tilting [10]. The etalon effect did not disappear completely, possibly because of residual reflection by scattering or because the tilting angle was insufficient. At the same time, tilting the sample introduces a longer optical path and produces blurring of the image, especially for thicker samples. Another way to reduce the etalon effect consists in placing a partially absorbing medium inside the etalon that is causing problems. Doing so will reduce the total usable power to a fraction f but will also reduce the etalon effect to roughly f^2, which means overall suppression of the interference term relative to the mean intensity to a fraction f.

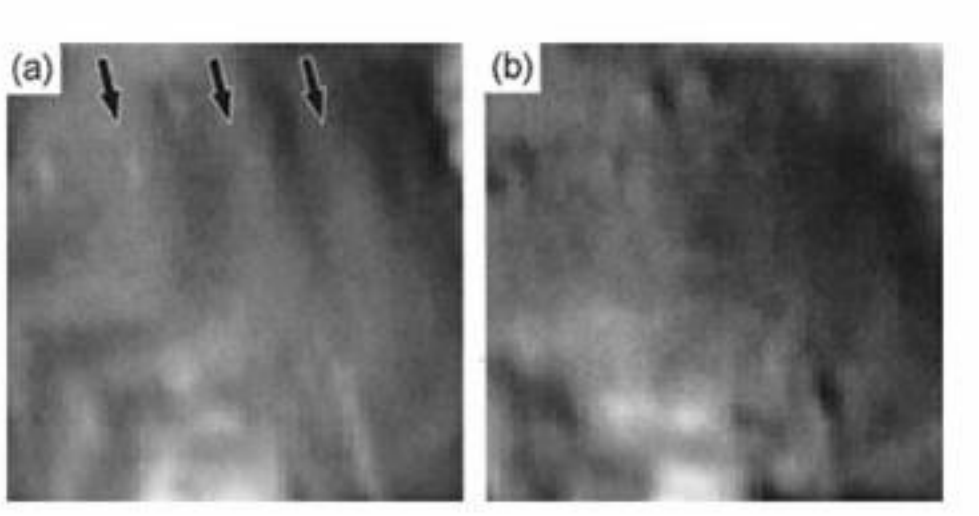

Figure 18: Reduction of the etalon effect by tilting the sample.
(a) The first scan is made in the normal horizontal position, and the resultant image exhibits fringes as indicated by arrows.
(b) For the second scan the sample was tilted at a 27° angle. The visibility of the interference fringes was clearly reduced.

5.1.3 Other Effects

Some of the other effects are mentioned below:

- Sample needs to be aligned in focus of the optical system; else the image becomes blurred. Thus, losing the spatial resolution.
- Particles in the environment tend to diffract the source radiation thus creating artifacts in the final signal.
- In general, optical systems are highly dependant on alignment of the measurement systems. Therefore, maximum error is caused due to poor alignment.

5.2 Other Concerns and Challenges

Several challenges presented by generating and detecting THz waves are outlined as follows.

5.2.1 Absorption rates

This is perhaps the most challenging hurdle to imaging when the sample is far away. Water and other polar liquids present a high absorption rate for THz waves, on the order

of 150cm^{-1} at 1 THz [6] .The Fig. 19 depicts the absorption rates in water in the THz region at room temperature. This limits the depth at which THz waves can be effective because most THz applications rely on THz passing though the samples. The impressions, however, should not be that absorption of THz waves is a complete limiting factor and something that needs to be completely resolved. If it were not for differences in absorption rates some of the effectiveness of THz imaging would be lost. [4]

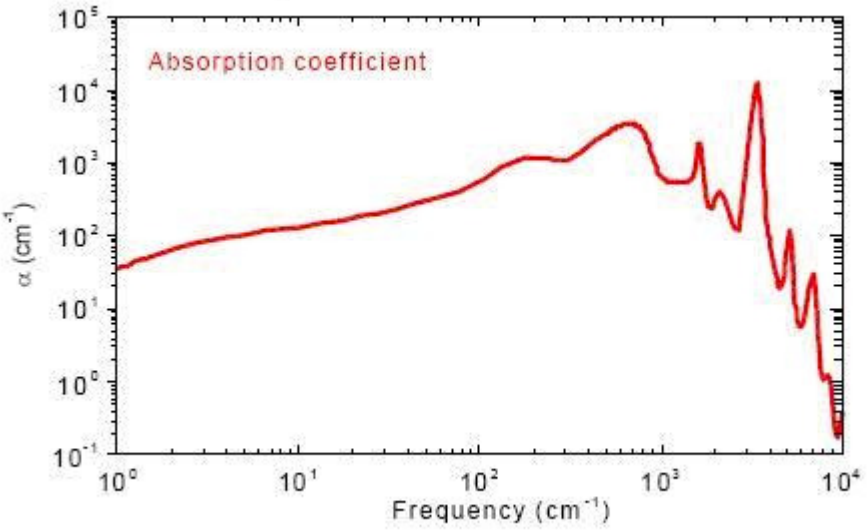

Figure 19: Absorption due to water in the THz region at room temperature.

5.2.2 Size and cost

A THz CW set up requires a few square meters. One possible simplification of the process is that the same semiconductor could be used to both generation and detection. This is because of the inverse relationship between optic rectification and electro-optic detection. This would allow transceivers to be made that are much smaller.

Currently the CW THz system employed cost in excess of $100K. Before the mainstream industrial community can adopt THz imaging the costs may have to reduce. More compact and inexpensive turn- key THz sources, detectors, and quasi-optical elements are under development, and are likely to bring system costs down to a few tens of thousands of dollars. Therefore, currently CW THz systems are limited to research application.

CHAPTER 6

CONCLUSION

THz measurement/imaging technology has proven to be a very valuable tool in fiber composites inspection. In particular, CW imaging systems are very attractive since they can be compact and easy to operate. However, the presence of the interference pattern in the normal reflection geometry may reduce the detection capabilities especially in thick samples. Implementing small angle reflection geometry may solve this problem but this will increase the size of the system and reduce the resolution. By far most optics systems face alignment related issues thus incorporating human error. Automation of alignment could prove very efficient.

In the fiber composites, THz imaging turn to be a promising solution to the problem of identifying and evaluating the presence of damage or defects and potentially increase safety and efficiency. In all cases, the resolution of the images is enough to detect the most important defects and the false rate calls is reduced because the images are easy recognizable to human vision. However, additional progress must be done to implement THz as effective tool. For instance, real-world application of these techniques requires speed as well as specificity. So far, the examples shown in this study utilize a raster scanning technique to form the images, wherein a THz beam is focused and scanned across the sample. For CW THz systems, combination with appropriate optics such detector arrays can be readily adapted to these applications.

CHAPTER 7

REFERENCES

[1] Brian Stephen Wong, Chua Fong Ming Ron, "Non-destructive testing of fiber reinforced composites and honeycomb structures." Nanyang Technological University, Singapore

[2] R. Glenn Wright, "Next Generation Terahertz Imaging System for Composite Material Assessment – Solution for Higher Quality and More Cost Efficient Composite Fabrication." GMA Industries, Inc.

[3] John Summerscales, "Non-Destructive Testing of Fibre-Reinforced Plastics Composites.", University of Plymouth

[4] THz Bridge, http://www.frascati.enea.it/THz-BRIDGE/database/spectra/searchdb.htm, December 2006.

[5] BRADLEY FERGUSON, XI-CHENG ZHANG, "Materials for terahertz science and technology.", REVIEW ARTICLE, nature materials , VOL 1 ,SEPTEMBER 2002

[6] X-C Zhang, "Terahertz wave imaging: horizons and hurdles.", Phys. Med. Biol. 47 (2002) 3667–3677

[7] G. Peter Swift, DeChang Daia, John R. Fletchera, Andrew J. Gallantb, James A. Levitta, Richard A. Abrama, Daryl M. Beggsa, Mikhail A. Kaliteevskia and J. Martyn Chamberlaina, "Terahertz scattering: comparison of a novel theoretical approach with experiment.", Terahertz and Gigahertz Electronics and Photonics V, Proc. of SPIE Vol. 6120, 61200R, (2005).

[8] TWI Knowledge, http://www.twi.co.uk/j32k/twiimages/ksijm001f1.gif, September 2006

[9] Advanced Photonix Website,http://www.advancedphotonix.com/ap_products/terahertz_whatis.asp, July 2006

[10] A. Dobroiu, M. Yamashita, Y. N. Ohshima, Y. Morita, C. Otani, and K. Kawase, " Terahertz Imaging System Based on a Backward-Wave Oscillator," Appl. Opt. 43, 5637-5646 (2004)